Electronic Supplementary Material (ESI) for Physical Chemistry Chemical Physics.

Supporting Information

Influence of Surface Area, Porous Structure, and Surface State on the Supercapacitor Performance of Titanium Oxynitride: Implications for Nanostructuring Strategy

Eun Joo Lee,[†,#] Lanlee Lee,[†,#] Muhammad Awais Abbas,[‡] and Jin Ho Bang[*,†,‡,§]*

Department of Bionano Technology, Department of Advanced Materials Engineering, and Department of Chemical and Molecular Engineering, Hanyang University, 55 Hanyangdaehak-ro, Sangnok-gu, Ansan, Gyeonggi-do 15588, Republic of Korea

AUTHOR INFORMATION

Corresponding Author: Jin Ho Bang

*Email: jbang@hanyang.ac.kr

[†] Department of Bionano Technology, Hanyang University

[‡] Department of Advanced Materials Engineering, Hanyang University

[§] Department of Chemical and Molecular Engineering, Hanyang University

[#] These authors contributed equally to this work.

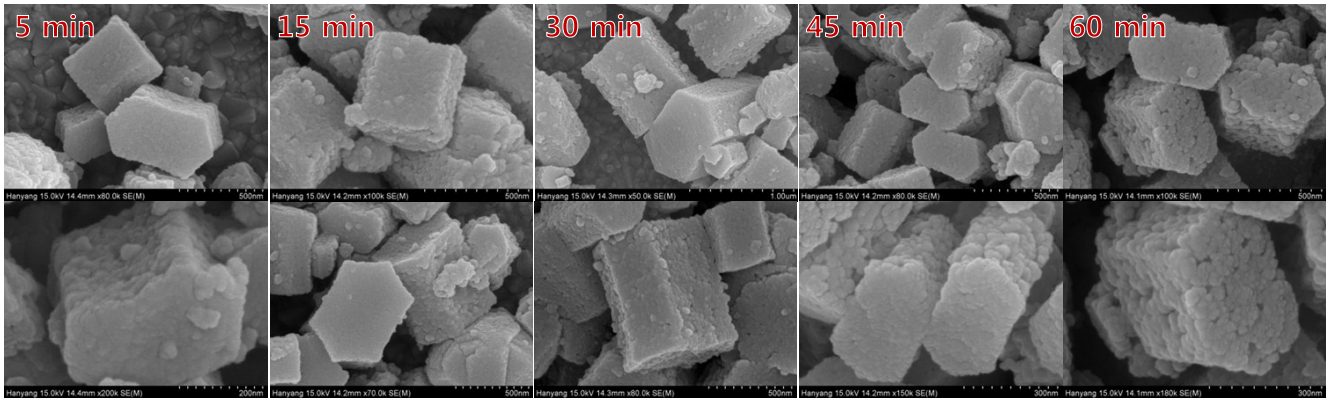

Figure S1. Time-resolved SEM images of h-TiO_xN_{1-x} at different NH_3 annealing times.

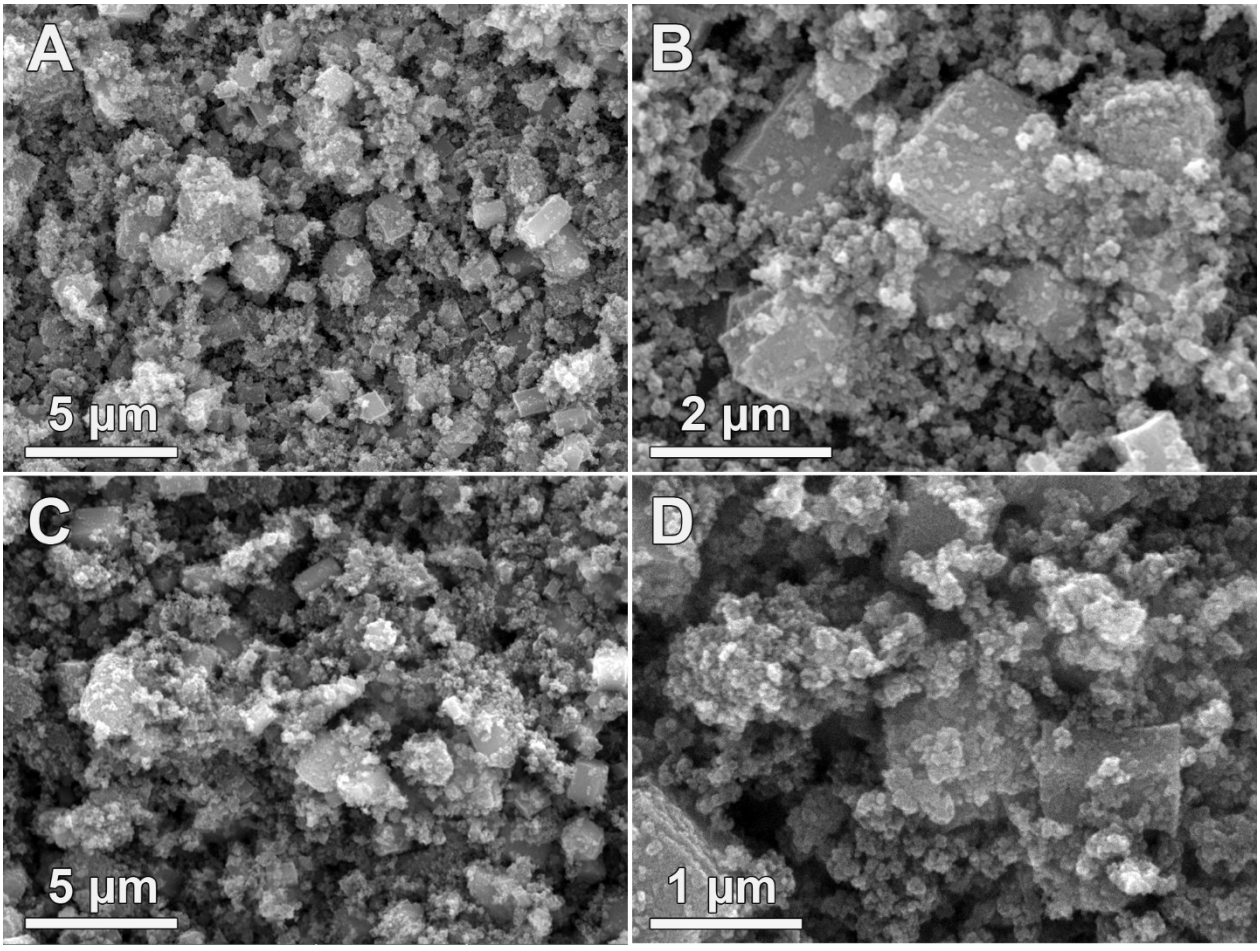

Figure S2. SEM images of h-TiO_xN_{1-x} obtained after (A and B) 2 h and (C and D) 3 h of nitridation.

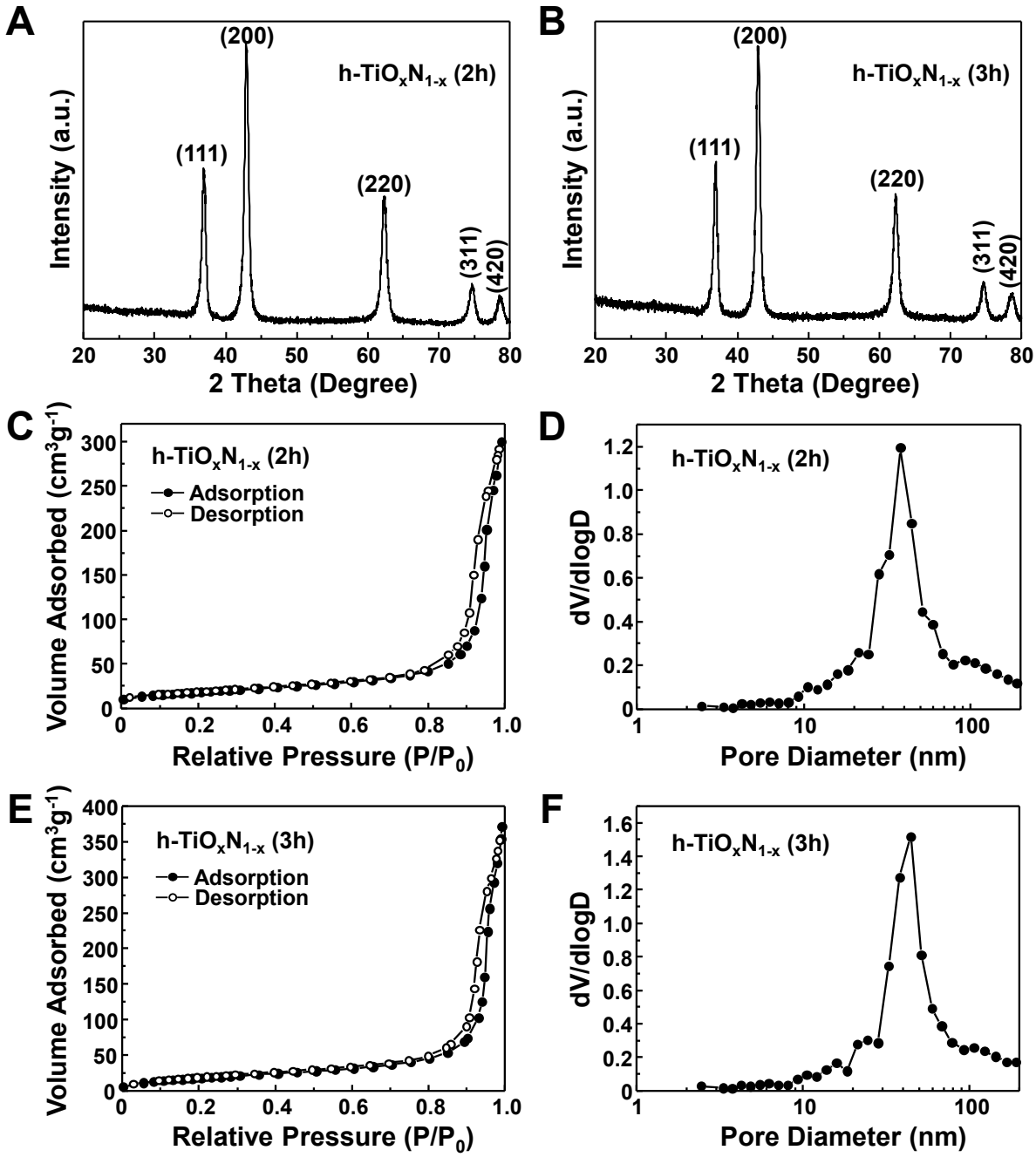

Figure S3. XRD patterns of h-TiO_xN_{1-x} obtained after (A) 2 h and (B) 3 h of nitridation. N_2 adsorption/desorption isotherms and the pore-size distribution of (C and D) h-TiO_xN_1 (2h) and (E and F) h-TiO_xN_1 (3h). The BET surface areas of h-TiO_xN_1 (2h) and of h-TiO_xN_1 (3h) are 64.5 and 68.6 m^2g^{-1} and their pore volumes are 0.461 and 0.549 cm^3g^{-1}, respectively. These increases in the surface area and pore volume as compared to those of h-TiO_xN_{1-x} obtained after 1 h of nitridation result from the partial collapse of the hexagonal secondary structure.

Table S1. Lattice parameters of TiO and TiN taken from JCPDS database. The red-colored JCPDS cards are the most commonly used ones in the literature. We too referred to these cards for the identification of our materials.

TiO			TiN	
JCPDS card number	Lattice parameter (Å)		JCPDS card number	Lattice parameter (Å)
04-004-9041	4.1705		04-002-0575	4.226
03-065-9473	4.1705		01-087-0632	4.234
01-089-5010	4.172		04-004-5181	4.235
01-089-3660	4.1735		04-002-0166	4.235
04-001-6834	4.174		01-074-8388	4.235
04-004-8994	4.1766		04-002-6279	4.2399
00-008-0117	4.177		04-004-6867	4.24
04-007-8198	4.177		04-003-1310	4.24
04-006-1351	4.177		04-004-0779	4.241
04-001-7607	4.178		04-003-1280	4.241
04-006-6021	4.179		04-001-2272	4.241
04-006-0746	4.18		00-038-1420	4.24173
04-004-4098	4.18		04-002-6734	4.242
04-002-5613	4.18		04-003-7146	4.243
04-002-5455	4.18		01-087-0629	4.244
04-002-0427	4.181		01-087-0628	4.244
01-072-2741	4.184		01-071-9845	4.2442
04-002-5596	4.185		04-003-3767	4.246
04-001-9372	4.185		04-002-2466	4.249
04-002-5624	4.19		04-002-5535	4.25
01-071-5272	4.2043		04-003-4495	4.26
04-003-5563	4.22		03-065-0965	4.27
01-072-4593	4.293		01-087-0631	4.32

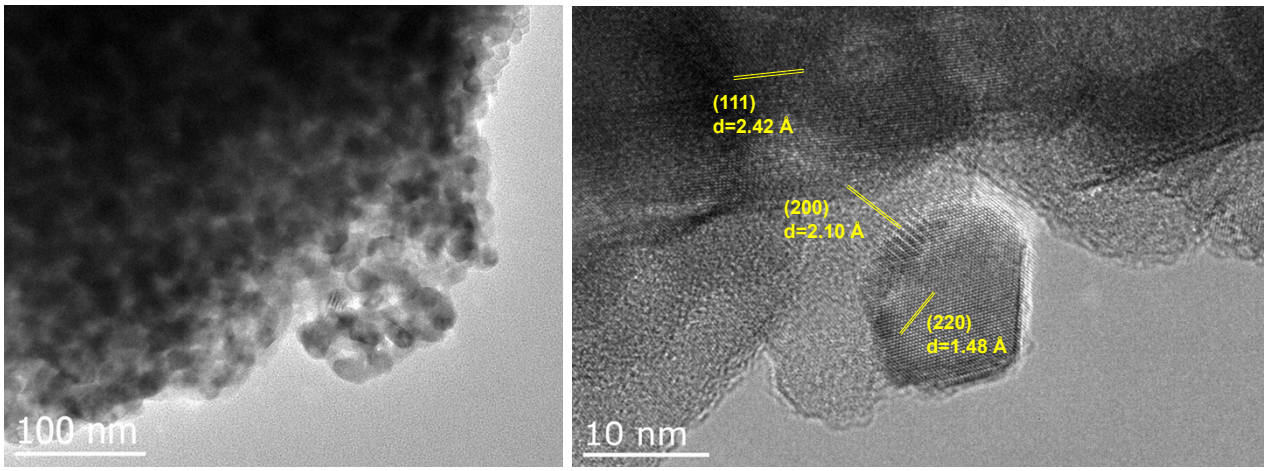

Figure S4. TEM images of h-TiO_xN_{1-x} at different magnifications.

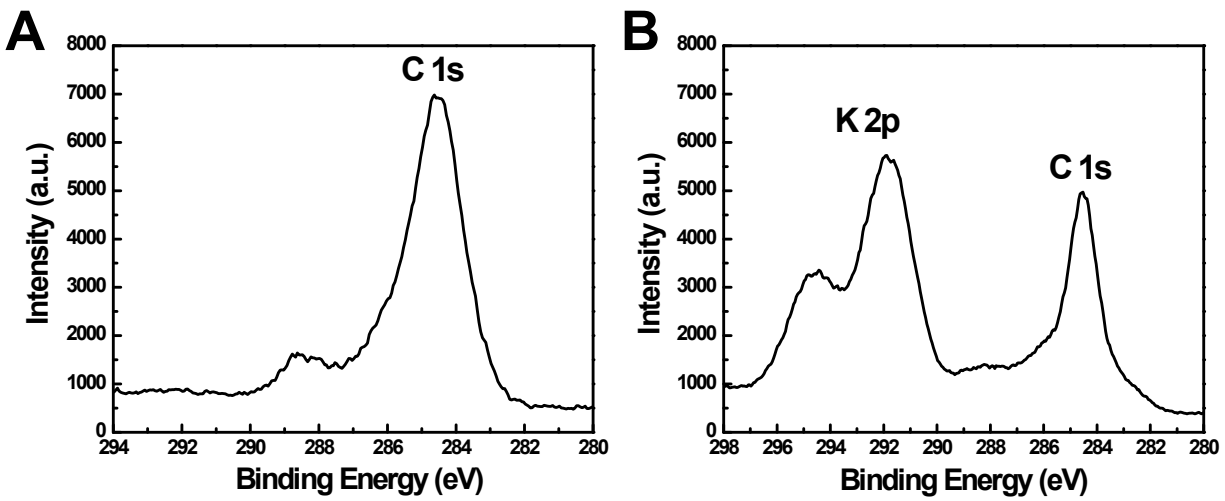

Figure S5. XPS C 1s and K 2p spectra of n-TiO_xN_{1-x} taken (A) before and (B) after 2000 cycles of potential sweep. The XPS measurements were carried out after thoroughly washing n-TiO_xN_{1-x} electrode to remove any possible ion residues on the surface.

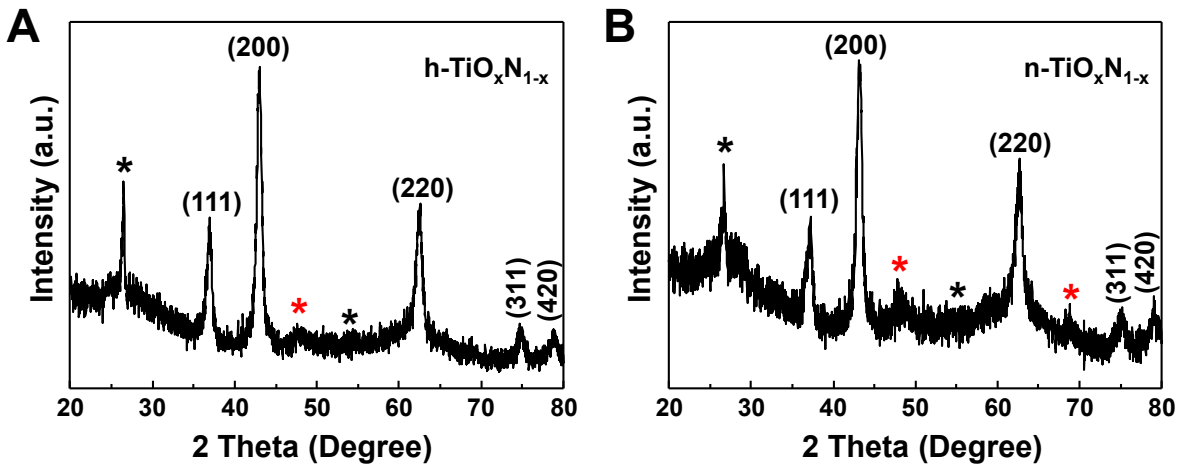

Figure S6. XRD patterns of (A) h-TiO_xN_{1-x} and (B) n-TiO_xN_{1-x} obtained after 2000 cycles of potential sweep. Note that the peaks labelled by the black-colored asterisks refer to diffraction peaks from carbon fiber paper used for an electrode substrate. Those by the red-colored asterisks are attributed to $K_2Ti_4O_9$ phase resulting from the corrosion of TiO_xN_{1-x}.

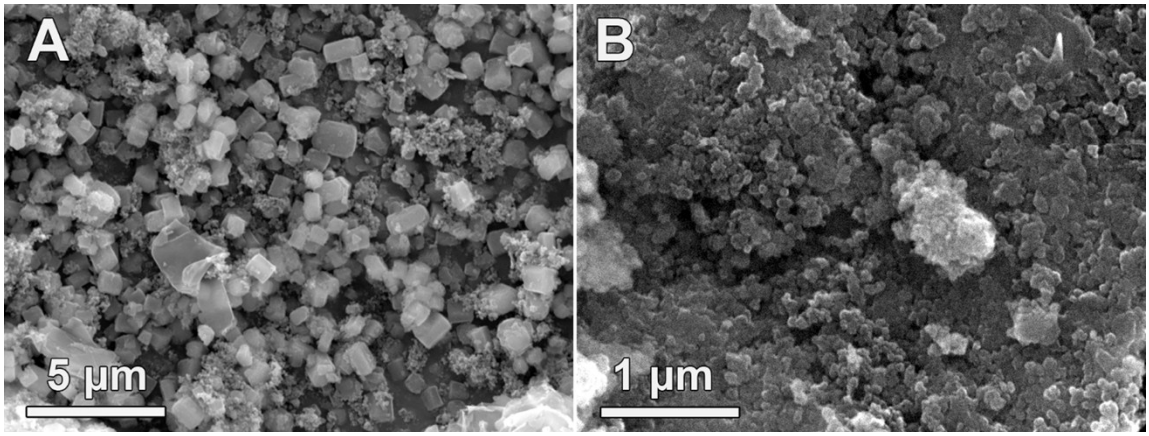

Figure S7. SEM images of (A) h-TiO_xN_{1-x} (small aggregated particles sporadically observed are carbon additive (Super P) used for the preparation of electrode paste) and (B) n-TiO_xN_{1-x} obtained after 2000 cycles of potential sweep. It is somewhat difficult to specifically discern n-TiO_xN_{1-x} from the mixture of n-TiO_xN_{1-x} and super P in the SEM image. However, given that the amount of n-TiO_xN_{1-x} used for the electrode (80 wt%) and the absence of well-defined surface morphology (i.e., severely deformed nanoparticle network) that are clearly visible in the SEM image of n-TiO_xN_{1-x} presented in Figs. 4A and 4B, we infer that the structural collapse was more facilitated in the n-TiO_xN_{1-x} than in h-TiO_xN_{1-x}.